Polygrammal Symmetries in Biomacromolecules: Heptagonal Poly *d* (As^4T) · poly *d* (As^4T) and Heptameric α-Hemolysin[a,b]

A. Janner[c]

Abstract

Polygrammal symmetries, which are scale-rotation transformations of star polygons, are considered in the heptagonal case. It is shown how one can get a faithful integral six-dimensional (6-D) representation leading to a crystallographic approach for structural properties of single molecules with a sevenfold point symmetry. Two biomacromolecules have been selected in order to demonstrate how these general concepts can be applied: the left-handed Z-DNA form of the nucleic acid poly *d* (As^4T) · poly *d* (As^4T), which has the line group symmetry 7_622, and the heptameric transmembrane pore protein *α*-hemolysin. Their molecular forms are consistent with the crystallo-graphic restrictions imposed on the combination of scaling transformations with sevenfold rotations. This all is presented in a two-dimensional (2-D) description, which is natural because of the axial symmetry.

Keywords

General crystallography • Molecular forms • Scale rotations • Poly *d* (As^4T) · poly *d* (As^4T) • *α*-hemolysin

Introduction

In a previous paper [1], a unifying general crystallography has been defined, characterized by the possibility of point groups of infinite order. Crystallography then becomes applicable even to single molecules, allowing a crystallographic interpretation of structural relations, which extend those commonly denoted as "*non-crystallographic*" in protein crystallography. In the same paper it is pointed out that molecular crystallography can be approached in a fairly similar way, as for quasicrystals. Alan Mackay, to whom this paper is dedicated on the occasion of his 75th anniversary, has given a pioneering and fundamental contribution to the problem of the relations between structure and symmetry in quasicrystals. For this occasion it seemed to me a good idea to focus attention on systems having a sevenfold point group symmetry.

Sevenfold self-similar quasicrystals, where crystallographic point groups of infinite order arise naturally, have been considered by various authors (see for some references [2–4]), but this field has not been developed because such quasicrystals have not been observed in nature. Observed in nature are, however, biomacromolecules with a rotation symmetry of order 7 and it is challenging to investigate the relevance of these point groups in the molecular case. A first attempt in this direction has been made for two hexagonal DNA's in terms of scaling properties of molecular forms reflecting an underlying point group of infinite order leaving the hexagonal lattice invariant [5]. In this paper, evidence is also given of similar behavior in B-DNA and in A-DNA,

[a] *Structural Chemistry* 2002, 13(3/4):277–287.

[b] This contribution is part of a collection entitled Generalized Crystallography and dedicated to the 75th anniversary of Professor Alan L. Mackay, FRS.

[c] Institute for Theoretical Physics, University of Nijmegen, Toernooiveld, Nijmegen 6525 ED, The Netherlands
e-mail: alo@sci.kun.nl

I. Hargittai, B. Hargittai (eds.), *Science of Crystal Structures: Highlights in Crystallography*,
DOI 10.1007/978-3-319-19827-9_7

which correspond to the tenfold and the elevenfold case, respectively.

It is essential to verify whether these scaling properties occur in nature as a rule rather than as an exception. From the point of view of molecular crystallography, this implies molecular forms with scaling factors critically related to the given point group symmetry. Typically, one should find τ, the golden mean, in the fivefold case, but this factor should be totally absent in the heptagonal case, because of the underlying number theoretical structure [4, 6].

The interest for the sevenfold case arose from the very nice axial view of α-hemolysin appearing in the cover picture of the book on Macromolecular Structures 1997 [7], which shows a nearly perfect sevenfold scalerotation symmetry of the heptamer. In order to distinguish between law and accident, nucleic acids have been considered as an alternative molecular case.

Nucleic acids occur as polynucleotides in different helical conformations, with a variety of axial symmetries. A full list of polynucleotides can be found in a historical survey of S. Arnott in the Oxford Handbook of Nucleic Acids edited by Neidle [8]. There, only one case is reported with sevenfold axial symmetry: the Z-DNA form of the left-handed poly $d(As^4T)\cdot$poly $d(As^4T)$ which, therefore, has been selected together with α-hemolysin. A third case, the double chaperonin (a larger and a smaller one) complexed with ADP and denoted as GroEl-GroES-$(ADP)_7$ will be discussed elsewhere. The analysis of the molecular forms is limited here to the prismatic forms of the backbone formed by the C_α's in the protein and disregarding hydrogen in the nucleic acid. The prismatic forms can be viewed along the sevenfold axis, allowing a two-dimensional (2-D) description of their three-dimensional (3-D) scale-rotational properties.

Many of the concepts raised so far are certainly nonfamiliar to most readers. Before developing the subject, a visualization of what one is talking about is, therefore, important. Polygrams and star polygons are first introduced, because these geometrical objects allow a simple approach to the symmetry of the various molecular forms. A *star polygon* denoted by the Schläfli symbol $\{n/m\}$ is obtained from a regular polygon by connecting each of the n vertices with its mth-subsequent one [9]. The regular polygon itself represents the trivial case $\{n/1\}$. A *polygram* consists of star polygons. Known for more than 2,000 years are the *pentagram* $\{5/2\}$ and the *hexagram* $\{6/2\}$. In the sevenfold case, in addition to the regular heptagon $\{7/1\}$, there are the two star heptagons $\{7/2\}$ and $\{7/3\}$ (Fig. 1). The other possible ones coincide with one of these.

The morphological role of these star polygons consists in relating regular heptagons of various size characterizing a molecular form. In particular, the central hole can very often be obtained from the external polygonal boundary enclosing the biomacromolecule by star polygons, as it has already been shown in the hexagonal case [5].

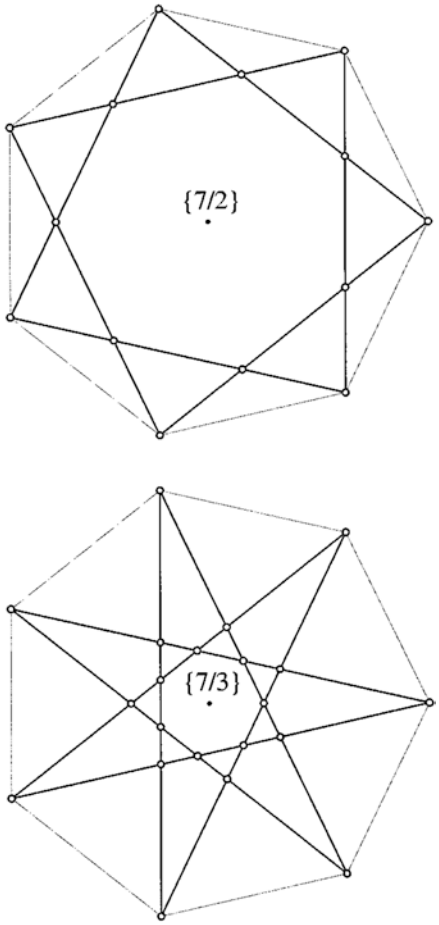

Fig. 1 The two regular heptagonal star polygons and their Schläfi symbol {7/2} and {7/3}.

In the case of α-hemolysin, the external boundary is a regular heptagon with vertices at the positions of the residue Glu71 in the cap domain of the seven chains, whereas the vertices of the central hole can be defined by the positions of the residue Lys147 of the transmembrane stem, which has the structure of a right-handed β-barrel. These boundaries are related by a $\{7/3\}$ star heptagon (Fig. 2). This implies that the two heptagons have the same orientation and that the axial distances of Glu71 and Lys147 are in the ratio $1{:}\mu$ determined by the symmetry of $\{7/3\}$, with $\mu=\cos(3\pi/7)/\cos(\pi/7)=0.2469\ldots$.

The structure of poly $d(As^4T)\cdot$poly $d(As^4T)$ projected along the helical axis is dominated by relations expressible in terms of $\{7/2\}$ star heptagons. The central molecular hole (due to s^4T, where s^4T indicates that the oxygen in the position 4 of the thymine is replaced by a sulfur atom) is so small with respect to the external heptagonal boundary, that at this stage no reliable scaling factor can be derived from polygrammal relations. Therefore, only the molecular form of the A subsystem is presented here (Fig. 3). One sees that,

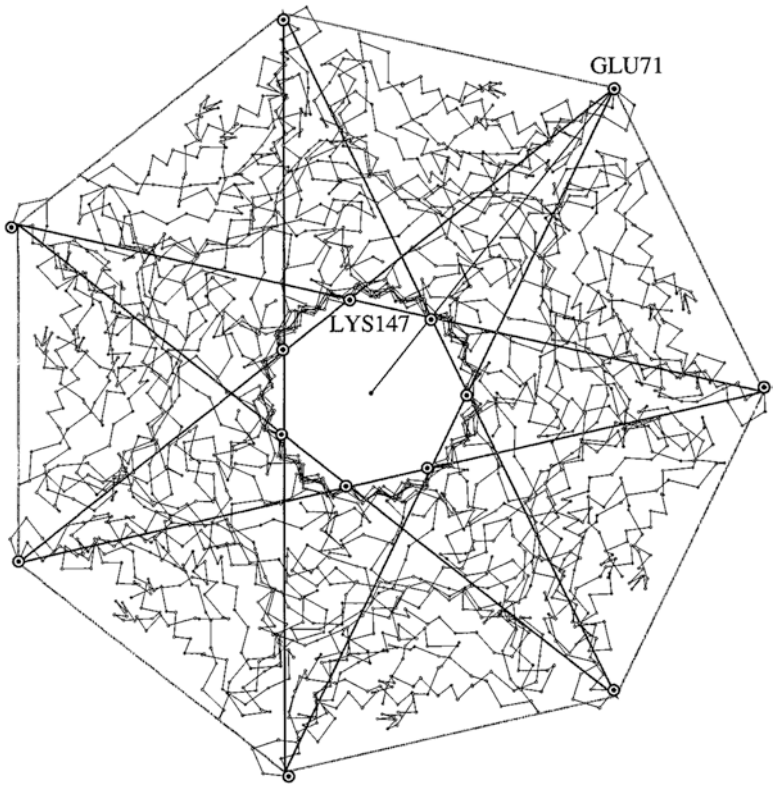

Fig. 2 Axial view of the heptameric protein α-hemolysin with a prismatic enclosing form. The two delimiting heptagons, with vertices at the projected positions of the residues Glu71 and Lys147, define the external boundary and the central hole, respectively. They are related by a scaling transformation with factor $\mu_3 = 0.2469\ldots$, which obeys the same crystallographic restriction as in the star heptagon {7/3}.

in this case, the central hole is scaled with respect to the external heptagon by a factor $-\mu_1^2$ with $\mu_1 = \cos(2\pi/7)/\cos(\pi/7) = 0.6920\ldots$. The minus sign implies that the two heptagons are in reverse orientation.

Following these preliminary observations, in the next section, an outline is given of a crystallographic characterization of star heptagons. In the other two sections, the molecular forms of α-hemolysin and of poly d(As⁴T) · poly d(As⁴T) are analyzed further. Additional morphological features (like the elliptic holes recognizable in Fig. 3) are discussed on the basis of crystallographic linear scalings, which are dilations (or contractions) in a given direction only.

Crystallography of Star Heptagons

The symmetry of a regular heptagon is given by the 2-D point group $K_0 = 7mm$ generated by a rotation R of order 7 and a reflection m:

$$K_0 = \langle R, m \mid R^7 = m^2 = (Rm)^2 = 1 \rangle \tag{1}$$

The frame of general crystallography adopted here [1] requires a faithful integral representation Γ of K_0, whose minimal dimension, in the present case, is 6.

$$K_0 \simeq \Gamma(K_0) \subset GL(6, \mathbb{Z}) \tag{2}$$

Where $\simeq$ denotes group isomorphism. This representation can be obtained by applying R and m to six of the seven radial vectors $a_1, a_2, \ldots, a_7$ of the heptagon. The orientation chosen is with a_7 along the positive direction of the x axis, and with the other ak as basis a for the representation Γ: $a = \{a_1, a_2, \ldots, a_6\}$. This basis is linearly dependent in the real R, but linearly independent in the rational integers Z. The components of these vectors with respect to an orthonormal basis $e = \{e_1, e_2\}$, with e_1 and e_2 in the direction of the x and y axis, respectively, are given by:

$$a_k = a_0 \left[\cos(k\varphi), \sin(k\varphi) \right], \quad \varphi = \frac{2\pi}{7} \quad \text{and} \quad k = 1, 2, \ldots, 6 \tag{3}$$

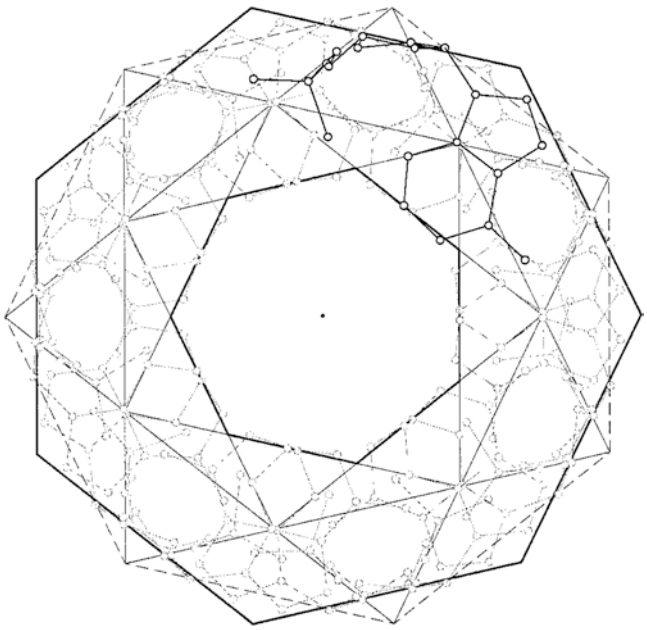

Fig. 3 Axial view of the A subsystem of the nucleic acid poly d(As^{4}T)·poly d(As^{4}T) in a Z-DNA conformation. As in the previous figure, the external heptagon (delimited by the sugar) and the central hole (due to the adenine) are in a scaling relation, which obeys a crystallographic restriction, as revealed by the star heptagons {7/2} inserted. The negative value of scaling factor $-\mu_1^2$, with $\mu_1 = 0.692\ldots$, implies that the central hole and the external boundary have a reverse orientation.

The representation matrices of the generators are then given by:

$$R(a) = \begin{pmatrix} 0 & 0 & 0 & 0 & 0 & -1 \\ 1 & 0 & 0 & 0 & 0 & -1 \\ 0 & 1 & 0 & 0 & 0 & -1 \\ 0 & 0 & 1 & 0 & 0 & -1 \\ 0 & 0 & 0 & 1 & 0 & -1 \\ 0 & 0 & 0 & 0 & 1 & -1 \end{pmatrix}$$
$$m(a) = \begin{pmatrix} 0 & 0 & 0 & 0 & 0 & 1 \\ 0 & 0 & 0 & 0 & 1 & 0 \\ 0 & 0 & 0 & 1 & 0 & 0 \\ 0 & 0 & 1 & 0 & 0 & 0 \\ 0 & 1 & 0 & 0 & 0 & 0 \\ 1 & 0 & 0 & 0 & 0 & 0 \end{pmatrix} \quad (4)$$

By considering $R(a)$ and $m(a)$ as orthogonal transformations R_s and m_s in a 6-D Euclidean space (the so-called *superspace*) one gets a formulation equivalent to a higherdimensional crystallography. Indeed, R_s and m_s leave invariant a

Table 1 Character table of the point group D_7 ($\varphi = 2\pi/7$)

D_7	ε	α, α^{-1}	α^2, α^{-2}	α^3, α^{-3}	$\beta\alpha^k$
$\Gamma^{(1)}$	1	1	1	1	1
$\Gamma^{(2)}$	1	1	1	1	−1
$\Gamma^{(3)}$	2	2cos φ	2cos 3φ	2cos 3φ	0
$\Gamma^{(4)}$	2	2cos 2φ	2cos 3φ	2cos φ	0
$\Gamma^{(5)}$	2	2cos 3φ	2cos φ	2cos 2φ	0

6-D lattice Σ, spanned in the superspace by a basis $a^s = \{a_1^s, a_2^s, \ldots, a_6^s\}$, with metric tensor

$$g_{ii}^s = 6, \quad g_{ik}^s = -1 \quad \text{for} \quad i \neq k \quad (5)$$

left invariant by R_s and m_s. The projection $\pi : a_k^s \to a_k$ maps the lattice Σ into the Z -module $M = \langle a_1, a_2, \ldots, a_6 \simeq \mathbb{Z}^6 \rangle$, of all integral linear combinations of these basis vectors. Accordingly, K_0 leaves M invariant: $K_0 M = M$.

The relation between the two bases a and as can be derived from the decomposition of the representation Γ into irreducible components. Looking at the character table of $D_7 \simeq 7m$ (Table 1) one finds:

$$\Gamma = \Gamma^{(3)} \oplus \Gamma^{(4)} \oplus \Gamma^{(5)} \quad (6)$$

where

$$\Gamma^{(3)}(\alpha) = R(e), \Gamma^{(4)}(\alpha) = R^2(e), \Gamma^{(5)}(\alpha) = R^3(e)$$
$$\Gamma^{(3)}(\beta) = \Gamma^{(4)}(\beta) = \Gamma^{(5)}(\beta) = m(e) \quad (7)$$

with α and β the two generators of the abstract group D_7, as in Table 1, and e denoting the 2-D orthonormal basis introduced above. This implies the following embedding of the basis a in the 6-D basis as:

$$\begin{aligned} a_1^s &= (a_1, a_2, a_3) \quad a_4^s = (a_4, a_1, a_5) \\ a_2^s &= (a_2, a_4, a_6) \quad a_5^s = (a_5, a_3, a_1) \\ a_3^s &= (a_3, a_6, a_2) \quad a_6^s = (a_6, a_5, a_4). \end{aligned} \quad (8)$$

Making use of the 2-D metrical relations between the elements of the basis a (with indices taken modulo 7):

$$a_i a_{i+k} = a_0^2 \cos(k\varphi) \quad (9)$$

one verifies that the basis a^s form, indeed, the R_s-invariant metric tensor $(a_0^2/2)g^s$. The orthogonal projection π considered above from the superspace to the heptagonal plane and with corresponds to the homomorphism $\Gamma(K_0) \to \Gamma^{(3)}(K_0)$, is given by:

$$\pi \ a_k^s = a_k, \quad k = 1, 2, \ldots, 6. \quad (10)$$

The idea on which a molecular crystallography approach is based is that there are possibly hidden molecular structural relations expressible as additional transformations leaving the Z -module M invariant. In the present case, this is indeed the case for the radial scaling symmetries of a self-similar

star heptagon (obtained from a starting regular heptagon by successive direct and inverse star constructions).

In the case {7/2} the radial scaling transformation $S_{-\mu 1}$:

$$S_{-\mu 1}(a)=\begin{pmatrix} 2 & -2 & 1 & 0 & -1 & 1 \\ 0 & 0 & -1 & 1 & -1 & 1 \\ 2 & -2 & 1 & -1 & 0 & 1 \\ 1 & 0 & -1 & 1 & -2 & 2 \\ 1 & -1 & 1 & -1 & 0 & 0 \\ 2 & -1 & 0 & 1 & -2 & 2 \end{pmatrix} \tag{11}$$

has a negative scaling factor $-\mu_1$ with

$$\mu_1 = -1+2\cos\varphi-2\cos 2\varphi = 0.692021\ldots, \quad \varphi = 2\pi/7 \tag{12}$$

In the case {7/3}, there are two radial scaling transformations, with scaling factors indicated by $-\mu_2$ and μ_3, respectively

$$S_{-\mu_2}(a)=\begin{pmatrix} 1 & 1 & -2 & 0 & 2 & -1 \\ 0 & 2 & -1 & -2 & 2 & 1 \\ -1 & 1 & 0 & -1 & 0 & 1 \\ 1 & 0 & -1 & 0 & 1 & -1 \\ 1 & 2 & -2 & -1 & 2 & 0 \\ -1 & 2 & 0 & -2 & 1 & 1 \end{pmatrix},$$
$$S_{\mu_3}(a)=\begin{pmatrix} -2 & 1 & 0 & 0 & 0 & -1 \\ 0 & -1 & 1 & 0 & 0 & -1 \\ -1 & 1 & -1 & 1 & 0 & -1 \\ -1 & 0 & 1 & - & 1 & -1 \\ -1 & 0 & 0 & 1 & -1 & 0 \\ -1 & 0 & 0 & 0 & 1 & -2 \end{pmatrix} \tag{13}$$

where:

$$\mu_2 = 2\cos\varphi+4\cos 2\varphi = 0.35689\ldots,$$

and

$$\mu_3 = -1+2\cos\varphi = 0.24697\ldots \tag{14}$$

These additional transformations allow the extension of the original Euclidean point group K_0 to infinite order, in a way still leaving the Z -module M invariant:

$$K_{\{7/2\}} = \langle R, m, S_{-\mu_1}\rangle, \quad K_{\{7/3\}} = \langle R, m, S_{-\mu_2}, S_{\mu_3}\rangle \tag{15}$$

Note the relations:

$$S_{-\mu} = -S_{\mu} \quad \text{and} \quad S_{-\mu_3} = S_{-\mu_1}S_{-\mu_2} \tag{16}$$

In a heptagram, however, the points at the intersection of the two different star polygons {7/2} and {7/3} have also to be considered for characterizing its self-similar symmetry. These points cannot be obtained by radial scaling from the heptagon considered but have, nevertheless, also integral coordinates (in the a basis). The reason is that they follow from integral linear scalings X_λ, Y_λ along the x and the y axis, respectively, whose product is a radial scaling radial scaling S_λ with the same scaling factor λ. This is a property that the radial scalings considered, so far, do not have. For fixing the ideas, consider a point P with coordinates $P(e)=(x, y)$. Then, for these linear scaling transformations one has:

$$X_\lambda(x, y)=(\lambda x, y), \quad Y_\lambda(x, y)=(x, \lambda y), \quad S_\lambda(x, y)=\lambda(x, y) \tag{17}$$

In particular, there are two sets of linear transformations ensuring the equivalence of the additional points with the previous ones:

$$X_{\mu_4}(a)=\begin{pmatrix} -4 & 3 & -1 & -1 & 3 & -5 \\ -1 & 1 & 0 & 0 & 0 & -1 \\ -3 & 2 & 0 & -1 & 2 & -3 \\ -3 & 2 & -1 & 0 & 2 & -3 \\ -1 & 0 & 0 & 0 & 1 & -1 \\ -5 & 3 & -1 & -1 & 3 & -4 \end{pmatrix},$$
$$Y_{\mu_4}(a)=\begin{pmatrix} 0 & 1 & -1 & 1 & -1 & 1 \\ 1 & -1 & 2 & -2 & 2 & -1 \\ -1 & 2 & -2 & 3 & -2 & 1 \\ 1 & -2 & 3 & -2 & 2 & -1 \\ -1 & 2 & -2 & 2 & -1 & 1 \\ 1 & -1 & 1 & -1 & 1 & 0 \end{pmatrix} \tag{18}$$

$$X_{-\mu_5}(a)=\begin{pmatrix} 0 & -3 & 2 & 2 & -3 & -1 \\ -1 & -7 & 3 & 3 & -5 & -1 \\ 0 & -1 & 1 & 0 & -1 & 0 \\ 0 & -1 & 0 & 1 & -1 & 0 \\ -1 & -5 & 3 & 3 & -4 & -1 \\ -1 & -3 & 2 & 2 & -3 & 0 \end{pmatrix},$$
$$Y_{-\mu_5}(a)=\begin{pmatrix} -2 & 1 & 2 & -2 & -1 & 3 \\ 1 & 0 & -1 & 1 & 1 & -1 \\ 2 & -1 & -1 & 2 & 1 & -2 \\ -2 & 1 & 2 & -1 & -1 & 2 \\ -1 & 1 & 1 & -1 & 0 & 1 \\ 3 & -1 & -2 & 2 & 1 & -2 \end{pmatrix} \tag{19}$$

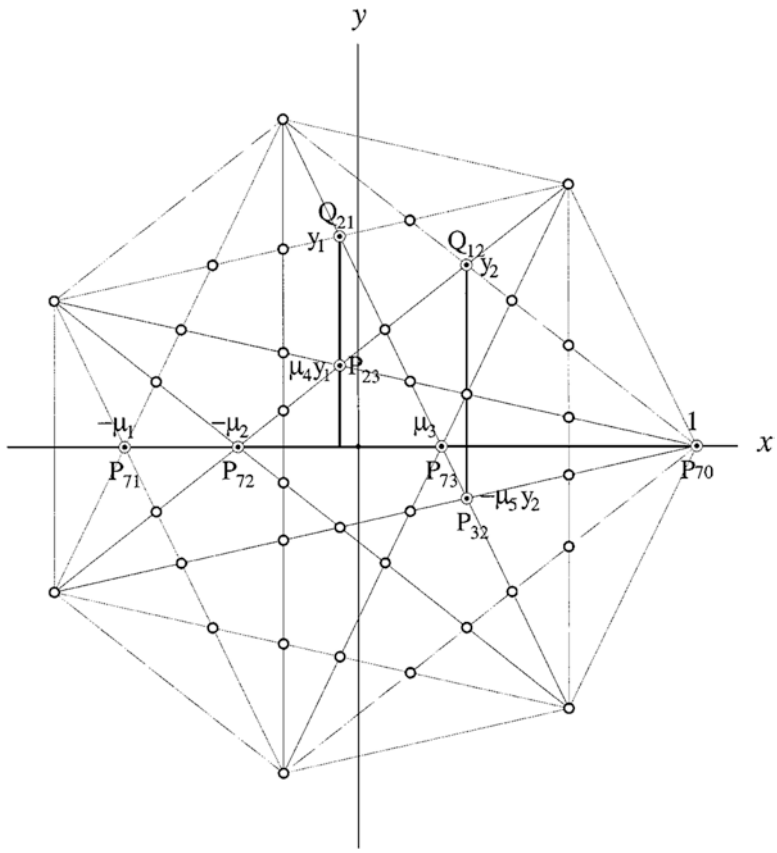

Fig. 4 Labeling convention of the intersections point in a heptagram consisting of the two star polygons {7/2} and {7/3} with examples of their mutual scaling relations. Thus, P_{71}, P_{72}, and P_{73} are obtained from P_{70} by radial scaling transformations S_{μ_i}, with scaling factors $-\mu_1$, $-\mu_2$, $-\mu_3$, respectively, whereas linear scalings Y_{μ_j} along the y axis and with factors μ_4 and $-\mu_5$, relate correspondingly Q_{21} with P_{23} and Q_{12} with P_{32}.

with scaling factors μ_4 and $-\mu_5$, where:

$$\begin{aligned}\mu_4 &= -3+4\cos\varphi-4\cos 2\varphi = 0.38404\ldots,\\ \mu_5 &= 1-4\cos\varphi-8\cos 2\varphi = 0.28620\ldots\end{aligned} \tag{20}$$

Note that $X_{-\lambda}\neq -X_\lambda$ and so also for $Y_{-\lambda}$.

These results allow the expression of all the intersection points of a heptagram as integral linear combination of the basis vectors and to assign to each point a set of *integral indices*, which are the components of the corresponding position vectors expressed in the basis a:

$$P(a)=(n_1,n_2,\ldots,n_6)$$

with

$$P=\sum_{k=1}^{6} n_k a_k \tag{21}$$

The following conventions for labeling the heptagrammal points have been adopted:

$$\begin{aligned}&P_{ik}=R^i P_{0k},\quad P_{ih}=S_{\mu_h} P_{i0},\quad k,h=1,2,3,\\ &i=1,2,\ldots,7\end{aligned}$$

$$\begin{aligned}&Q_{21}=Y_{\mu_4}^{-1}P_{23},\quad Q_{12}=Y_{-\mu_5}^{-1}P_{32},\\ &Q_{ij}=R^i Q_{oj},\qquad j=1,2\end{aligned} \tag{22}$$

where μ_h' denotes $(\pm)\mu_h$ taken with the appropriate sign. A relation between scaling factors and indices is visualized in Fig. 4. The missing indices are easily computed by applying $R^k(a)$ to those indicated. Table 2 gives the result.

The intersection points Q_{ij} of a heptagram represent one way to arrive at crystallographic linear scalings, but this way does not reveal their characteristic structural role. In order to find out the typical aspect, consider how the vertices of a regular heptagon (chosen in the x orientation) transform under the combination of linear scalings to first order X_λ, Y_λ, and the sevenfold rotations of the point group K_0 as in the double cosets $K_0\,X_\lambda\,K_0$ and $K_0\,Y_\lambda\,K_0$. The image points of the a_k one gets, all are on circles with center C_k at the mean distance between a_k and $S_\lambda\,a_k$, for $S_\lambda = X_\lambda\,Y_\lambda$. While X_λ gives rise to an off-center heptagon in the same x orientation, Y_λ yields an heptagon in the reverse orientation $-x$. Figure 5 illustrates these

Table 2 Indexed intersection points of the heptagram (see Fig. 4)

{7/1}	{7/2}	{7/3}	
P_{10} 100000	P_{11} 202112	P_{12} $10\bar{1}11\bar{1}$	P_{13} $\bar{2}0\bar{1}\bar{1}\bar{1}\bar{1}$
P_{20} 010000	P_{21} $\bar{2}0\bar{2}0\bar{1}\bar{1}$	P_{22} 121022	P_{23} $1\bar{1}1000$
P_{30} 001000	P_{31} $1\bar{1}1\bar{1}10$	P_{32} 210120	P_{33} $01\bar{1}100$
P_{40} 000100	P_{41} $01\bar{1}1\bar{1}1$	P_{42} $0\bar{2}\bar{1}0\bar{1}\bar{2}$	P_{43} $001\bar{1}10$
P_{50} 000010	P_{51} $\bar{1}\bar{1}0\bar{2}0\bar{2}$	P_{52} 220121	P_{53} $0001\bar{1}1$
P_{60} 000001	P_{61} 211202	P_{62} $\bar{1}11\bar{1}01$	P_{63} $\bar{1}\bar{1}\bar{1}\bar{1}0\bar{2}$
P_{70} $\bar{1}\bar{1}\bar{1}\bar{1}\bar{1}\bar{1}$	P_{71} $\bar{2}0\bar{1}\bar{1}0\bar{2}$	P_{72} $\bar{1}\bar{2}00\bar{2}\bar{1}$	P_{73} 211112
{7/2} ∩ {7/3}			
Q_{11} $010\bar{1}10$	Q_{21} $0010\bar{1}1$	Q_{31} $\bar{1}\bar{1}\bar{1}0\bar{1}\bar{2}$	Q_{41} 211121
Q_{51} $\bar{1}10001$	Q_{61} $\bar{1}\bar{2}0\bar{1}\bar{1}\bar{1}$	Q_{71} $10\bar{1}100$	
Q_{12} $\bar{1}\bar{1}\bar{1}0\bar{2}\bar{1}$	Q_{22} $10001\bar{1}$	Q_{32} 121112	Q_{42} $\bar{2}\bar{1}0\bar{1}\bar{1}\bar{1}$
Q_{52} $1\bar{1}0100$	Q_{62} $01\bar{1}010$	Q_{72} $001\bar{1}01$	

properties for the case $\lambda = \mu_4^{-1} = 2.60388\ldots$ given above. The presence of off-center circles in the structure of a given molecular form strongly suggests the possible presence of linear scaling.

α-Hemolysin

α-Hemolysin is a heptameric transmembrane pore protein. The data for the atomic coordinates have been taken from PDB 7AHL by Song et al. [10]. The structure consists of seven chains labeled *A* to *G*. Before projecting the structure along the axis, the original data have been oriented and centered using the positions of the residue Glu71 in the chains *A*, *D*, *F*. The corresponding prismatic molecular form has already been presented in the introduction (Fig. 2).

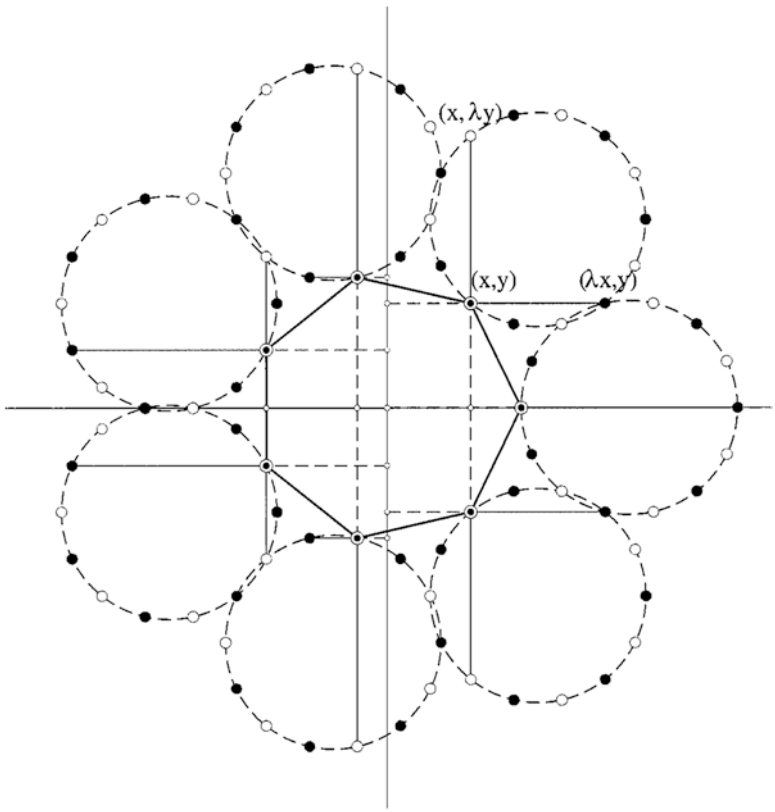

Fig. 5 Off-center circles obtained by applying linear scalings with given scaling factor to the vertices of a regular heptagon. Indicated is how the (x, y) coordinates of these points are transformed by X_λ and Y_λ to $(\lambda x, y)$ and $(x, \lambda y)$, respectively. The remaining points follow from the sevenfold rotational symmetry (leading to conjugated linear scalings $R^k X_\lambda R^{-k}$ and $R^k Y_\lambda R^{-k}$). Here, the scaling factor $\lambda = \mu_4^{-1} = 2.60388\ldots$ ensures that the matrices $X_\lambda(a)$ and $Y_\lambda(a)$ are integral, so that all these points can be indexed by integers.

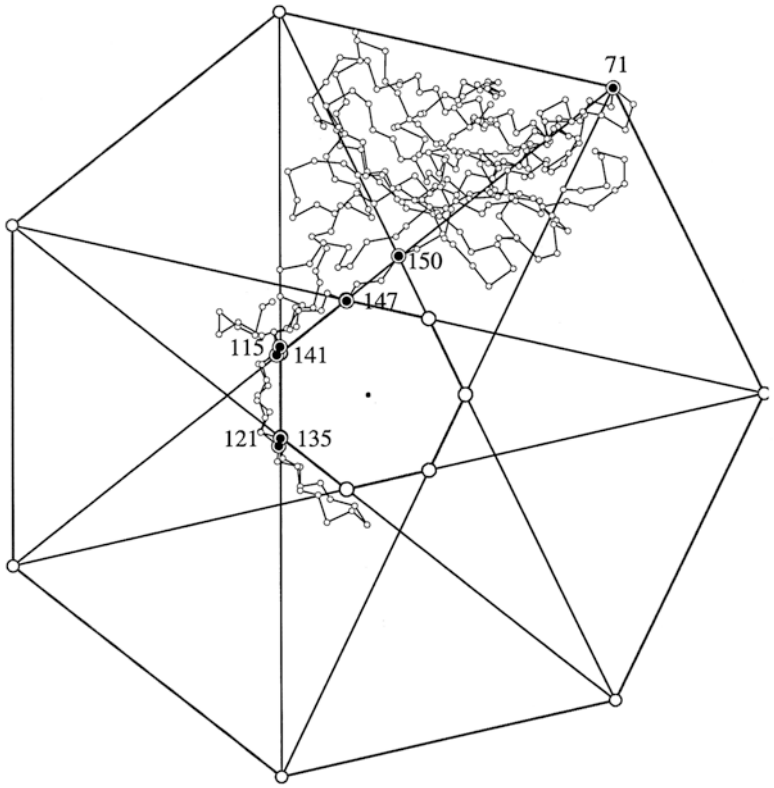

Fig. 6 A protomer of α-hemolysin is shown in a view along the central axis of the heptamer and in relation with the star heptagon {7/3} fitted at the position of the residue 71. The projected positions of a number of other residues (150, 147, 141, 135, 121, and 115) at points of the star heptagon are an indication that the protomer folds in a way predisposed not only to the sevenfold rotational symmetry (in the stem domain), but also to crystallographic scale rotations, which relate the stem domain with the cap domain, in a way still requiring further investigation.

The projection of a single chain shows that the scalerotation symmetry of the star polygon {7/3}, which characterizes the molecular form of the heptamer, is already predisposed in the folding of the monomer (Fig. 6). One sees that, in addition to the residues 71 and 147 indicated in Fig. 2, several more (150, 141, 135, 121, and 115) also fit fairly well with the intersection points of the star heptagon. The corresponding scale-rotation transformations, however, do not connect atomic positions, but only vertical lines (parallel to the central axis) through these positions. This does not exclude the possibility of a 3-D point group relating these same positions. In the spirit of molecular crystallography, one even expects the existence of such a group, which would explain the molecular form observed, but this investigation has not yet been carried out. From the molecular form one finds some evidence for additional linear scaling, but not strong enough to be presented here.

Poly *d*(As^{4}T)·poly *d*(As^{4}T)

The left-handed double helix formed by the two strands of poly d(As^{4}T)·poly d(As^{4}T) is characterized by a dinucleotide repeat with line group symmetry $7_6 22$ of which the details have been reported in *Nature* [11]. The corresponding data are listed as structure No. 16 in a survey by Chandrasekaran and Arnott, published in a volume of the Landolt-Börstein collection [12].

It is convenient to first consider the molecular form of each nucleotide subsystem separately. The form of the A-subsystem has already been presented in the introduction (Fig. 3), that of the s^{4}T subsystem is shown in Fig. 7. Both share the absolute value of scaling factor $\mu_1 = 0.6920\ldots$ of the star heptagon {7/2}, but not always the corresponding negative sign. This implies that the successively scaled heptagons may have the same or the reverse orientation. While in the case of adenine the central hole is already reached at the second contraction

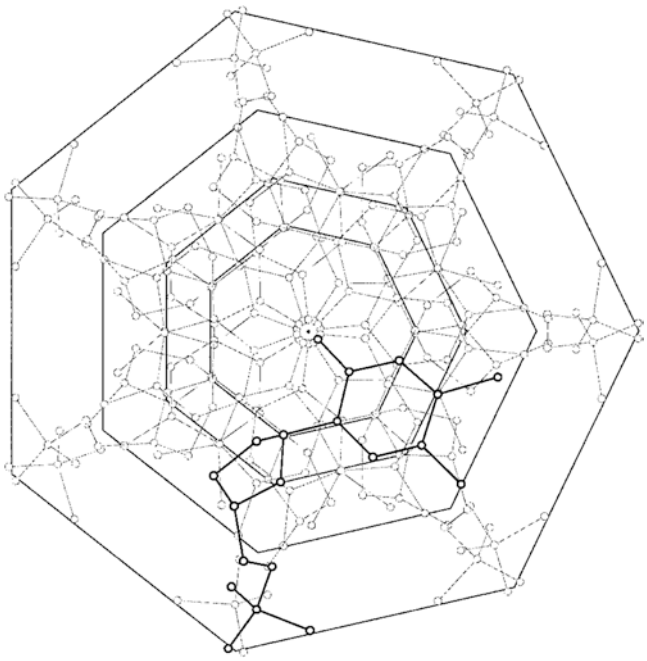

Fig. 7 Prismatic molecular form of the s^4T subsystem in poly d(As^4T) · poly d(As^4T) viewed along the helical axis. Shown are successive internal boundaries scaled from the external heptagon by μ_1, μ_1^2, μ_1^3, respectively, where $\mu_1 = 0.6920\ldots$ is the same factor on which the star heptagon {7/2} is based and which also plays a role in the A subsystem (Fig. 3). In the present case, the central hole and the external boundary are not related by a scaling factor obeying crystallographic restrictions. (See also Fig. 10).

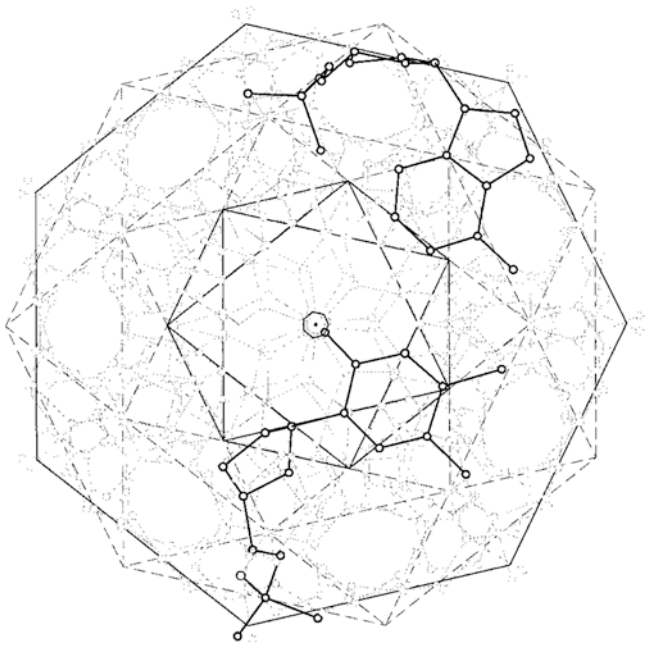

Fig. 8 Molecular form adopted for the (As^4T) system of poly d(As^4T) · poly d(As^4T), with the sugar of the A nucleotide delimiting the external boundary, leaving outside oxygens of the phosphate of the s^4T nucleotide. Despite this mismatch, the overall structure is still compatible with internal prismatic boundaries base on {7/2} star polygons.

level, that of the thymine is not simply scaled by a power of μ_1. The heptagons scaled by μ_1, μ_1^2, μ_1^3, show, however, the expected compatibility with morphological features.

This general behavior is confirmed when combining the two subsystems in the molecular form of the dinucleotide shown in Fig. 8. As the external boundaries of the two subsystems are slightly different in size, the combination requires an adaptation. The one of the A subsystem gives the best fitting for the whole, despite the fact that two of the phosphate oxygens of the s^4T nucleotide are no more inside the heptagon of the external boundary. The morphological importance of the star heptagon {7/2} is confirmed.

Looking at Fig. 8, one recognizes elliptically shaped holes tangent to the external heptagon at midedge positions. As already pointed out in the introduction, this indicates the possible presence of linear scalings which, as explained in the second, can give rise to off-center circular structures. In the present case, the natural candidates are the two linear scaling transformations X_{μ_1}, Y_{μ_1} whose product gives the radial scaling S_{μ_1}. These linear scalings have not been considered so far because they not integral in the heptagonal basis *a*. However, the appearance of midedge heptagonal

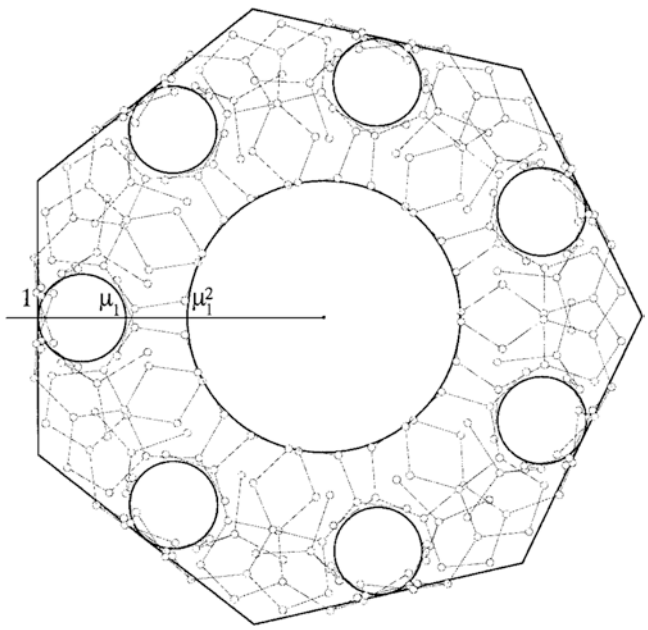

Fig. 9 The elliptical holes visible in the molecular form of the A subsystem (as shown in Fig. 3) are obtained as off-center circles from linear scalings X_{μ_1}, Y_{μ_1} (and their *R*-conjugated ones) applied to the midedges of the external heptagon, in the same way as illustrate in Fig. 5, but now for $\mu_1 = 0.692\ldots$ One sees that the central hole then follows by a further radial scaling transformation S_{μ_1}, and this is unexpected.

points with half-integer indices, suggests a corresponding centering of the 6-D lattice, leading to half-integers in the entries of the linear scaling when expressed in what one could denote as the conventional basis a. One finds indeed:

$$X_{\mu_1}(a) = \begin{pmatrix} -3/2 & 3/2 & -1/2 & -1/2 & 3/2 & -5/2 \\ -1/2 & 1 & 0 & 0 & 0 & -1/2 \\ -3/2 & 1 & 1/2 & -1/2 & 1 & -3/2 \\ -3/2 & 1 & -1/2 & 1/2 & 1 & -3/2 \\ -1/2 & 0 & 0 & 0 & 1 & -1/2 \\ -5/2 & 3/2 & -1/2 & -1/2 & 3/2 & -3/2 \end{pmatrix} \quad (23)$$

$$Y_{\mu_1}(a) = \begin{pmatrix} 1/2 & 1/2 & -1/2 & 1/2 & -1/2 & 1/2 \\ 1/2 & 0 & 1 & -1 & 1 & -1/2 \\ -1/2 & 1 & -1/2 & 3/2 & -1 & 1/2 \\ 1/2 & -1 & 3/2 & -1/2 & 1 & -1/2 \\ -1/2 & 1 & -1 & 1 & 0 & 1/2 \\ 1/2 & -1/2 & 1/2 & -1/2 & 1/2 & 1/2 \end{pmatrix} \quad (24)$$

with positive scaling factor $\mu_1 = 0.6920\ldots$. The off-center holes of the A subsystem are fairly well approximates by applying these linear scaling transformations to the mid-edges of the external heptagon, as shown in Fig. 9. Moreover, the central hole can also be described by a circle, which is a factor μ_1^2 smaller than the one inscribed in the heptagon. One could also start from the central hole and arrive at the off-center hole observed by applying the inverse radial scaling $S_{\mu_1}^{-1}$ first, and then the corresponding linear dilation $X_{\mu_1}^{-1}$, $Y_{\mu_1}^{-1}$ in combination with the appropriate sevenfold rotations.

This last interpretation opens the door to a corresponding characterization of the molecular form of the s^{4}T subsystem, as represented in Fig. 10. Starting from the heptagon of the central hole with vertices at a mean O2 position of diadically related thymine molecules, one gets by a radial scaling $S_{\mu_1}^{-4}$ the heptagon formed by the corresponding mean C1 positions, and by a further $S_{\mu_1}^{-3}$ transformation those corresponding to the C6 ones. From this last heptagon, one obtains the circular off-center holes by the linear transformations $X_{\mu_1}^{-2}$, $Y_{\mu_1}^{-2}$ squares of the dilations given above. These off-center circles are thus related to the central hole by elements X_{μ_1}, Y_{μ_1}, R, and m of the point group, but no simple relation could be found with the heptagon delimiting the molecular form. The reason is perhaps that this heptagon does not represent the relevant molecular envelop for the s^{4}T subsystem. This would explain why in this case there is no crystallographic scaling transformation relating the central hole and the external heptagon, as it is the case for the A subsystem.

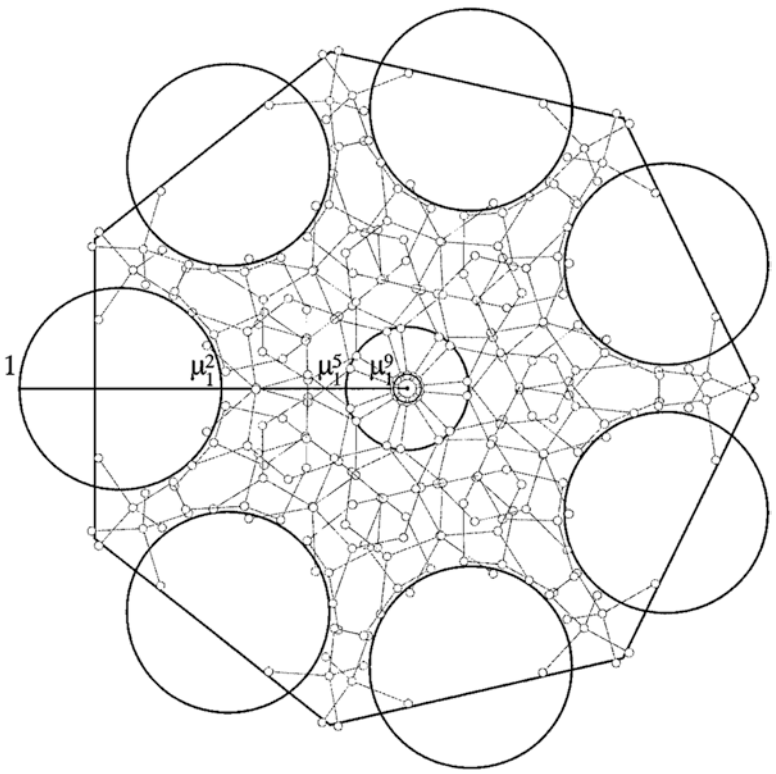

Fig. 10 The same linear scalings as in Fig. 9 allow to find a better envelop for the s^{4}T subsystem than the regular heptagon. Now successive radial scalings $S_{\mu_1}^3$ and $S_{\mu_1}^4$ relate this curved boundary to the internal circular ones through the C1 and the O2 positions of the thymine, respectively. The latter positions define the central hole.

Acknowledgments Thanks are expressed to R. Chandrasekaran for kindly having made available to the author the structural data of poly d(As^4T) · poly d(As^4T) reported in Landolt-Börstein; to R. de Gelder and to B. Souvignier for pertinent remarks and valuable suggestions. Stimulating discussions with C. W. Hilbers are gratefully acknowledged. The graphical program XPS used has been originally designed by J. M. Thijssen.

References

1. Janner, A. *Acta Crystallogr*. **2001,** *A57*, 378.
2. Nischke, K.-P.; Danzer, L. *Discrete Comp. Geom*. **1996,** *15*, 221. (See also Materialien/Preprints LXXIX, University of Bielefeld, 1994.)
3. Barache, D. Ph. D. Thesis, University of Paris 7, 1995.
4. Gazeau, J. P. In *Symmetry and Structural Properties of Condensed Matter*; Lulek, T.; Florek, W.; Walcerz, S., Eds.; World Scientific: Singapore, 1995; p. 369.
5. Janner, A. *Crystal Eng*. **2001,** *4*, 119.
6. Janner, A. In *GROUP21 Physical Applications and Mathematical Aspects of Geometry*, *Groups and Algebras*.; Doebner, H.-D.; Scherer, W.; Schulte, C., Eds.; World Scientific: Singapore, 1997; p. 949.
7. Hendrickson, Wayne A.; Wüthrich, Kurt. *Macromolecular Structures 1997. Atomic Structures of Biological Macromolecules Reported during 1996*; Current Biology Ltd.: London, 1997.
8. Arnott, S. In *Oxford Handbook of Nucleic Acid Structure*; Neidle S., Ed.; Oxford University Press: Oxford, 1998; p. 1.
9. Coxeter, H. S. M. *Introduction to Geometry*; Wiley: New York, 1961.
10. Song, L.; Hobaugh, M. R.; Shustak, C.; Cheley, S.; Bayley, H.; Gouaux, J. E. *Science* **1996,** *274*, 1859.
11. Arnott, S.; Chandrasekaran, R.; Birdsall, D. L.; Leslie, A. G. W.; Ratliff, R. L. *Nature* (*London*) **1980,** *283*, 743.
12. Chandrasekaran, R.; Arnott, S. In *Landolt-Börstein Numerical Data and Functional Relationships in Science and Technology* (*Group VII*, *Biophysics*); Springer: Berlin, 1989; Vol. VII, 1b, p. 31.